This is an open access article published under a Creative Commons Attribution (CC-BY) License, which permits unrestricted use, distribution and reproduction in any medium, provided the author and source are cited.

analytical chemistry

Technical Note

Cite This: Anal. Chem. 2018, 90, 12372−12376

pubs.acs.org/ac

Proteins on Supported Lipid Bilayers Diffusing around Proteins Fixed on Acrylate Anchors

Bianca Buchegger,[§] Johannes Kreutzer,[§,†] Markus Axmann,[⊥] Sandra Mayr,[¶] Richard Wollhofen,[§] Birgit Plochberger,[¶] Jaroslaw Jacak,[*,§,¶] and Thomas A. Klar[§]

[§]Institute of Applied Physics, Johannes Kepler University Linz, Altenberger Straße 69, 4040 Linz, Austria

[¶]School of Medical Engineering and Applied Social Sciences, University of Applied Sciences Upper Austria, Garnisonstraße 21, 4020 Linz, Austria

[⊥]Institute of Medical Chemistry, Center for Pathobiochemistry and Genetics, Medical University of Vienna, Währinger Straße 10, 1090 Vienna, Austria

Supporting Information

ABSTRACT: Mobility of proteins and lipids plays a major role in physiological processes. Platforms which were developed to study protein interaction between immobilized and mobile proteins suffer from shortcomings such as fluorescence quenching or complicated fabrication methods. Here we report a versatile platform comprising immobilized histidine-tagged proteins and biotinylated proteins in a mobile phase. Importantly, multiphoton photolithography was used for easy and fast fabrication of the platform and allows, in principle, extension of its application to three dimensions. The platform, which is made up of functionalized polymer structures embedded in a mobile lipid bilayer, shows low background fluorescence and allows for mobility of arbitrary proteins.

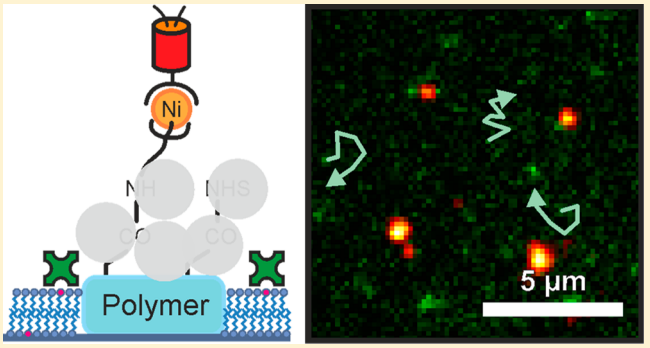

Restrictions in lateral mobility of lipids and proteins in the cell membrane have significant impact on physiological processes. Cell−cell interactions, protein binding, cell signaling, and molecular transport, for example, depend on the mobility of cells and proteins.[1−6] Migration or accumulation of proteins and lipids in cell membranes leads to membrane heterogeneities which effect biochemical processes and mechanical properties of membranes.[7] One possibility to mimic such heterogeneities is the construction of artificial platforms which allow separation of two mobile phases or the introduction of a mobile and an immobile phase. In the past, introduction of barriers within an artificial lipid bilayer was realized by using different micro- and nanostructures made of polymers, alumina, gold or TiO_2,[8−10] chromium,[11] nanoimprinting of albumin,[12] patterning substrates with femtosecond lasers,[13] scanning probe lithography,[14] or nanopatterned graphene.[15] Furthermore, platforms comprising two different mobile phases were demonstrated.[11,16] These geometrically confined supported lipid bilayers found application in studying physiological processes e.g. in leukemia cell studies,[17] T cell signaling,[18−20] or the phosphorylation of the epidermal growth factor.[21]

In addition to membrane proteins with mobility around the nanopatterned substrates, fixed proteins anchored to the substrate via well-defined linkers are equally important for physiological studies. Such anchoring can be achieved, for instance, via dip-pen nanolithography,[22] gold nanoparticles,[23,24] nanoimprint lithography,[25,26] e-beam lithography,[27,28] or multiphoton and stimulated emission depletion (STED) nanolithography.[29,30] Physiological applications comprise integrin activation for focal adhesion sites,[23,31] studies on T cell organization and signaling,[32,33] or investigations of lipid organization in ordered domains in living cells.[34]

The natural extension of applying either mobile proteins on lipid membranes or proteins fixed to micro- and nanostructures on a substrate is to use a hybrid protein platform providing both phases, a mobile one flowing around a fixed one. This was anticipated by Kung et al.,[12] Smith et al.,[13] and Shi et al.[14] although only demonstrated for inactive albumin as fixed protein. Some important physiological studies using functional fixed and functional mobile proteins were reported recently. The groups of Groves and Salaita for example studied epidermal growth factors on breast cancer cells,[35−37] while most recently T cell receptor triggering was successfully investigated by using a hybrid platform.[38] In most of these studies gold nanoparticles were used to tie down the proteins in the fixed phase,[35,36,38] with the disadvantage of fluorescence

Received: June 8, 2018
Accepted: October 16, 2018
Published: October 16, 2018

© 2018 American Chemical Society

DOI: 10.1021/acs.analchem.8b02588
Anal. Chem. 2018, 90, 12372−12376

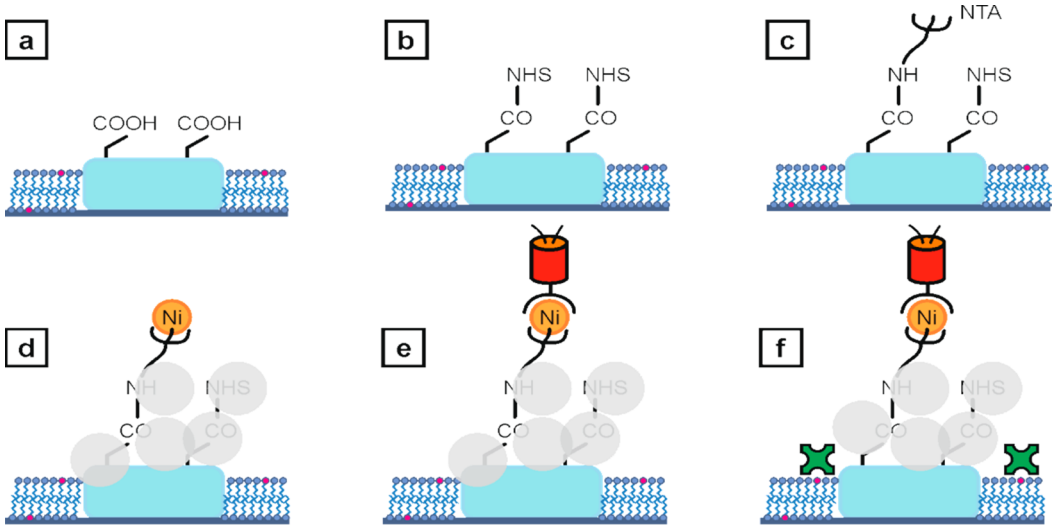

Figure 1. a) Polymer anchors with carboxy-functionality surrounded by a supported lipid bilayer spiked with a biotin-modified lipid (pink). b) NHS groups covalently bound to the carboxy groups. c) NH_2−NTA bound to the NHS-functional polymer structure. d) Albumin (light gray circles) blocks the remaining carboxy groups and NHS esters. This step prevents unspecific protein binding to the polymer anchors. Subsequently, the NTA head groups are chelated with nickel ions. e) Immobilization of histidine-tagged fluorescent proteins. f) Streptavidin-Alexa Fluor 555 was adhered to the biotinylated lipid bilayer. All schemes are not to scale.

quenching by gold particles which hampers optical readout.[39] Although very small protein anchors of ∼6 nm can be realized, self-assembly of gold nanoparticles as used by Lohmüller et al.[35,36] or Deeg et al.[40] is limited to periodic, mostly hexagonal patterns. TiO_2 circumvents fluorescence quenching,[10] but the self-assembled pattern is again hexagonal. Other techniques, which overcome the disadvantages of inflexibility in pattern design, were applied but show shortcomings in fabrication speed and cost. E-beam lithography[38] for example provides full flexibility in two and 2.5 dimensions but is a cost intensive technique, while dip-pen lithography[37] shows limited flexibility and is a rather slow fabrication method. Clearly, there is a demand for alternative hybrid platforms comprising mobile and immobile proteins which show full flexibility in platform design as well as fast and cheap fabrication and ideally account for excellent optical readout. This is especially of interest, since the present physiological studies are just the beginning of possible applications.

In this Technical Note, we demonstrate a versatile hybrid platform which allows pinning of two different proteins, one in a mobile lipid bilayer and one immobilized on polymer nanostructures. Importantly, the nanostructures are fabricated by multiphoton photolithography (MPP)[41,42] which allows for cheap and fast processing and, in principle, extension of the platform in three dimensions.[43] The polymer structures are written by MPP in a functional acrylate resin and serve as anchor points for arbitrary histidine-tagged proteins. The mobile phase in which the acrylate structures are embedded is made of a biotin spiked lipid bilayer and can be loaded with arbitrary biotinylated proteins. Thus, the two different immobilization mechanisms via histidine tags on the immobile phase and the streptavidin bound to the biotinylated lipid bilayer allow for orthogonal immobilization of proteins. Additionally, the polymer structure is transparent and shows negligible background fluorescence, which facilitates optical readout.

EXPERIMENTAL SECTION

MPP allows for maskless fabrication of two- and three-dimensional polymer structures with feature sizes down to 100 nm[41,42,44−46] and a lateral resolution around 200 nm.[47] Carboxy-functional polymer structures can be written using a photoresist consisting of a carboxy-modified acrylate and a photoinitiator.[48] The monomers are pentaerythritol triacrylate (PETA, Sigma-Aldrich Co., USA) and 20 wt % 2-carboxyethyl acrylate (CEA, Sigma-Aldrich Co., USA). One wt % Irgacure 819 (IC 819, BASF Schweiz AG, Switzerland) was added as photoinitiator. For control measurements, structures without carboxy-functionality were fabricated using pure PETA with 1 wt % of IC 819. The chemical structures of the photoresist ingredients as well as detailed information about the experimental design and the sample preparation can be found in the Supporting Information.

After fabrication and development, the polymer structures were cleaned by rinsing with ethanol and incubation with ethylenediaminetetraacetic acid buffer. 1-palmitoyl-2-oleoyl-sn-glycero-3-phosphocholine vesicles (POPC, Avanti Polar Lipids Inc., USA)[49,30] with 4 wt % of 1,2-dipalmitoyl-*sn*-glycero-3-phosphoethanolamine-N (cap biotinyl) (sodium salt) (16:0 Biotinyl Cap PE, Avanti Polar Lipids Inc., USA) were sonicated for 20 min and incubated for another 20 min, leading to a biotin-modified supported lipid bilayer enclosing but not covering the previously fabricated polymer anchors (see Figure 1a).[8,30,48,50,51] After washing with 4-(2-hydroxyethyl)-1-piperazineethanesulfonic acid (HEPES) buffer (pH 7.5, 50 mM), the carboxy groups on the polymer anchors were converted to N-hydroxysuccinimide (NHS) esters (Figure 1b). After a second washing step, amino-labeled nitrilotriacetic acid (NH_2−NTA) was covalently bound to the NHS esters (Figure 1c). After further washing, an aqueous solution of nickel(II) chloride was added.[28,52,53] To ensure binding specificity of histidine-tags to Ni-NTA, the eventually remaining carboxy groups and NHS esters were blocked using albumin. The chelation of nickel ions and the passivation with albumin is shown in Figure 1d. Subsequently, we added histidine-tagged

DOI: 10.1021/acs.analchem.8b02588
Anal. Chem. 2018, 90, 12372−12376

photoswitchable monomeric protein orange (PSmOrange) (Figure 1e) or histidine-tagged emerald green fluorescent protein (EmGFP). Then, fluorescently labeled streptavidin was added and attached to the biotin within the lipid bilayer (Figure 1f).[54] The immobilization of histidine-tagged EmGFP or PSmOrange to the carboxy-functional acrylate structure via Ni-NTA interaction as well as binding of Alexa Fluor 555 labeled streptavidin to the lipid bilayer was analyzed via fluorescence microscopy using excitation wavelengths of 491 nm, 642 nm, and 532 nm, respectively. The photoinitiator IC 819 used in writing the polymer structures shows a negligible fluorescence signal at excitation with 491 nm, 532 nm, or 642 nm.[30] The chemical structures of the molecules used for protein anchoring can be found in the Supporting Information.

RESULTS AND DISCUSSION

Protein Immobilization. The selectivity of histidine-tag mediated protein binding via Ni-NTA to carboxy-functional acrylate structures is shown by comparing EmGFP binding to polymer grids with and without carboxy-functionality, offset by half a period in both lateral directions (see the scanning electron microscope (SEM) image in Figure 2a). The polymer lines have line widths of about 130 nm. The weak fluorescence signal of the polymer lines fabricated with pure PETA stems from autofluorescence of the structure and unspecifically bound proteins. Fluorescence of the Ni-NTA-functional polymer grid is about 10 times higher compared to the fluorescence from the pure PETA grid (Figure 2b). Additional data from control experiments are shown in the Supporting Information.

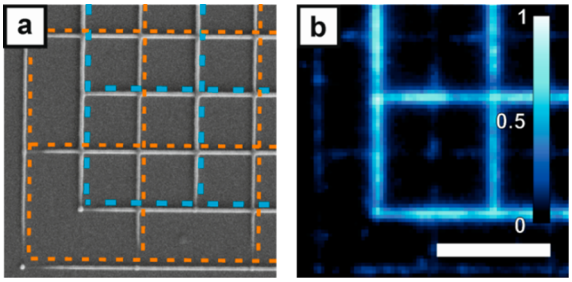

Figure 2. Specific anchoring of histidine-tagged proteins to Ni-NTA modified acrylate structures. a) SEM image of a nonfunctional grid (orange dashed lines) superimposed with a carboxy-functional one (blue dashed lines), offset by half a period in x and y directions. b) A fluorescence microscopy image of the same structure shows strong protein (EmGFP) binding to the Ni-NTA-functional structure but only weak binding to the pure PETA grid. Excitation wavelength 491 nm. The scale bar of 5 μm in (b) is valid for (a) and (b).

Hybrid Protein Platform. The carboxy-functional polymer anchors have diameters of about 100 nm. First, the fluorescent histidine-tagged protein PSmOrange was immobilized on polymer anchors following the strategy shown in Figure 1(a-e). Subsequently, streptavidin labeled with Alexa Fluor 555 was adhered to the biotin-spiked POPC bilayer as sketched in Figure 1f. Figure 3a shows a fluorescence image of the carboxy-acrylate dots with immobilized histidine-tagged PSmOrange (excitation wavelength 642 nm). The fluorescent proteins bind to the polymer anchors. Fluorescence from the Alexa Fluor 555 labeled streptavidin, adhered to the lipid bilayer, is shown in Figure 3b (excitation wavelength 532 nm). Figure 3c shows an overlay of both images. A movie of Alexa Fluor 555 labeled streptavidin diffusing around the fixed PSmOrange can be found in the Supporting Information. In order to quantify the two-dimensional movement of the streptavidin within the bilayer, trajectories were analyzed (Figure 3d). To determine the diffusion constant, a mean square displacement (MSD) statistic (Figure 3e) was applied. The diffusion constant was determined applying a two-dimensional model of free diffusion with $MSD(t) = MSD_0 + 4Dt$ (solid line), fitted using the first three points in the MSD(t) plot.[49] The resulting mean square displacement versus time plot yields a diffusion constant of $D = 0.38 \pm 0.09$ $\mu m^2/s$. The offset MSD_0 of the linear fit in the MSD(t)-plot corresponds to a positional accuracy of 193 nm.

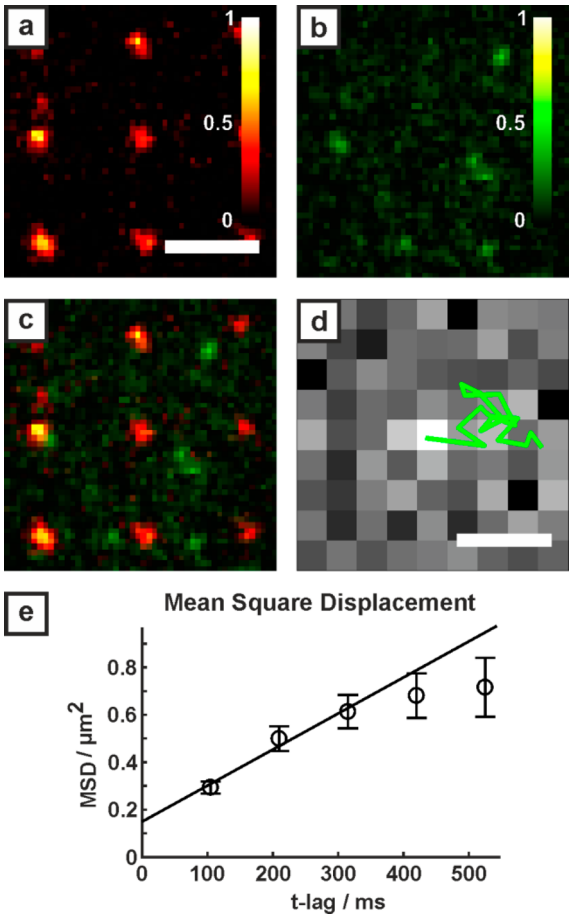

Figure 3. Hybrid protein platform. a) Fluorescence image of histidine-tagged PSmOrange anchored to the carboxy-functional polymer (642 nm excitation). b) Fluorescence of Alexa Fluor 555 tagged streptavidin adhered to the supported lipid bilayer (532 nm excitation). c) Snapshot of the merged red and green channels. A movie of streptavidin molecules flowing around fixed PSmOrange can be found in the Supporting Information. The scale bar of 3 μm in (a) is valid for (a-c). d) Trajectory (green) superimposed on the first fluorescence image of the molecule. Scale bar: 500 nm. e) Mean square displacement versus time for the Alexa Fluor 555 tagged streptavidin diffusing within the POPC lipid bilayer (number of traces = 125).

CONCLUSIONS

In conclusion, a platform for binding of two different proteins, one diffusing on a supported lipid bilayer and the other fixed to acrylate anchors, is presented. Two different types of fluorescent proteins (EmGFP or PSmOrange) were specifically

DOI: 10.1021/acs.analchem.8b02588
Anal. Chem. 2018, 90, 12372−12376

immobilized on acrylate structures of about 100 nm in size, bearing carboxy-functionality which is further converted to provide specific Ni-NTA/histidine-tag interaction. Another protein (Alexa Fluor 555 labeled streptavidin) is bound to a lipid bilayer, spiked with biotinylated lipids and surrounding the acrylate anchors. The streptavidin is moving within the lipid bilayer, flowing around the fixed fluorescent proteins. This two-component system, combining both, a mobile and an immobile fraction of different proteins, is well suited for the analysis of protein−protein interactions in living cells. Acrylate protein anchors show much less fluorescence quenching than gold nanoparticles, which have been used in previous platforms for two-phase protein binding. The versatile platform allows immobilization of any histidine-tagged protein to the NTA binding sites as well as incorporation of any biotinylated protein in the mobile phase.[55] Importantly, the histidine-tag and the biotin−streptavidin linkage is independent, hence binding of two different types of proteins, one mobile, one fixed, should be easily achievable for a wide range of physiological problems. This extends the applicability of this hybrid protein platform way beyond the two previously described examples of studies on epidermal growth factors[35−37] or T cell signaling.[38] In comparison to e.g. e-beam lithography, MPP is less cost-intensive and provides three-dimensional writing capability. Further, it is thinkable, that using STED lithography the structure size could be reduced to lateral sizes of around 60 nm.[48,56] The height of the polymer structures can be varied from 20 nm (MPP) down to 10 nm (STED lithography).[29] We previously showed that 80% of nanoanchors (size about 60 nm) can carry only one antibody.[29] Hence, an application for direct protein−protein interaction can be expected.

■ ASSOCIATED CONTENT

Supporting Information

The Supporting Information is available free of charge on the ACS Publications website at DOI: 10.1021/acs.analchem.8b02588.

Description of the experimental setups for fabrication and imaging, chemical structures of the photoresist components and sample preparation, chemical structures and materials for protein binding experiments, control experiments, and characterization of the supported lipid bilayer on differently treated substrates (PDF)

Movie of moving streptavidin proteins surrounding the immobilized histidine-tagged fluorescent proteins on polymer anchors (AVI)

■ AUTHOR INFORMATION

Corresponding Author

*E-mail: jaroslaw.jacak@fh-linz.at.

ORCID

Bianca Buchegger: 0000-0003-4346-8415

Jaroslaw Jacak: 0000-0002-4989-1276

Thomas A. Klar: 0000-0002-1339-5844

Present Address

†Department of Chemistry, Istanbul Technical University, 34469 Maslak, Istanbul, Turkey.

Notes

The authors declare no competing financial interest.

■ ACKNOWLEDGMENTS

We would like to thank Heidi Piglmayer-Brezina, Bernhard Fragner, and Alfred Nimmervoll for technical support. The work was funded by the Austrian Science Fund (FWF), project P26461 and Interreg ATCZ14. M.A. has been supported by Austrian Science Fund Project P29110-B21.

■ REFERENCES

(1) Vereb, G.; Szöllosi, J.; Matkó, J.; Nagy, P.; Farkas, T.; Vigh, L.; Mátyus, L.; Waldmann, T. A.; Damjanovich, S. *Proc. Natl. Acad. Sci. U.S.A.* **2003**, *100* (14), 8053−8058.

(2) Engel, A.; Gaub, H. E. *Annu. Rev. Biochem.* **2008**, *77*, 127−148.

(3) Snider, J.; Kittanakom, S.; Damjanovic, D.; Curak, J.; Wong, V.; Stagljar, I. *Nat. Protoc.* **2010**, *5* (7), 1281−1293.

(4) Engelman, D. M. *Nature* **2005**, *438* (7068), 578−580.

(5) Simons, K.; Ikonen, E. *Nature* **1997**, *387* (6633), 569−572.

(6) Cordwell, S. J.; Thingholm, T. E. *Proteomics* **2010**, *10* (4), 611−627.

(7) Damjanovich, S.; Gáspár, R.; Pieri, C. *Q. Rev. Biophys.* **1997**, *30* (1), 67−106.

(8) Groves, J. T.; Ulman, N.; Boxer, S. G. *Science* **1997**, *275* (5300), 651−653.

(9) Cai, H.; Wolfenson, H.; Depoil, D.; Dustin, M. L.; Sheetz, M. P.; Wind, S. J. *ACS Nano* **2016**, *10* (4), 4173−4183.

(10) Guasch, J.; Diemer, J.; Riahinezhad, H.; Neubauer, S.; Kessler, H.; Spatz, J. P. *Chem. Mater.* **2016**, *28* (6), 1806−1815.

(11) Jackson, B. L.; Groves, J. T. *J. Am. Chem. Soc.* **2004**, *126* (43), 13878−13879.

(12) Kung, L. A.; Kam, L.; Hovis, J. S.; Boxer, S. G. *Langmuir* **2000**, *16* (17), 6773−6776.

(13) Smith, A. M.; Huser, T.; Parikh, A. N. *J. Am. Chem. Soc.* **2007**, *129* (9), 2422−2423.

(14) Shi, J.; Chen, J.; Cremer, P. S. *J. Am. Chem. Soc.* **2008**, *130* (9), 2718−2719.

(15) Li, W.; Chung, J. K.; Lee, Y. K.; Groves, J. T. *Nano Lett.* **2016**, *16* (8), 5022−5026.

(16) Sekula, S.; Fuchs, J.; Weg-Remers, S.; Nagel, P.; Schuppler, S.; Fragala, J.; Theilacker, N.; Franzreb, M.; Wingren, C.; Ellmark, P.; Borrebaeck, C. A. K.; Mirkin, C. A.; Fuchs, H.; Lenhert, S. *Small* **2008**, *4* (10), 1785−1793.

(17) Wu, M.; Holowka, D.; Craighead, H. G.; Baird, B. *Proc. Natl. Acad. Sci. U.S.A.* **2004**, *101* (38), 13798−13803.

(18) Mossman, K. D.; Campi, G.; Groves, J. T.; Dustin, M. L. *Science* **2005**, *310* (5751), 1191−1193.

(19) DeMond, A. L.; Mossman, K. D.; Starr, T.; Dustin, M. L.; Groves, J. T. *Biophys. J.* **2008**, *94* (8), 3286−3292.

(20) Manz, B. N.; Jackson, B. L.; Petit, R. S.; Dustin, M. L.; Groves, J. *Proc. Natl. Acad. Sci. U.S.A.* **2011**, *108* (22), 9089−9094.

(21) Stabley, D.; Retterer, S.; Marshall, S.; Salaita, K. *Integr. Biol.* **2013**, *5* (4), 659−668.

(22) Lim, J.-H.; Ginger, D. S.; Lee, K.-B.; Heo, J.; Nam, J.-M.; Mirkin, C. A. *Angew. Chem., Int. Ed.* **2003**, *42* (20), 2309−2312.

(23) Cavalcanti-Adam, E. A.; Micoulet, A.; Blümmel, J.; Auernheimer, J.; Kessler, H.; Spatz, J. P. *Eur. J. Cell Biol.* **2006**, *85* (3−4), 219−224.

(24) Wolfram, T.; Belz, F.; Schoen, T.; Spatz, J. P. *Biointerphases* **2007**, *2* (1), 44−48.

(25) Falconnet, D.; Pasqui, D.; Park, S.; Eckert, R.; Schift, H.; Gobrecht, J.; Barbucci, R.; Textor, M. *Nano Lett.* **2004**, *4* (10), 1909−1914.

(26) Pla-Roca, M.; Fernandez, J. G.; Mills, C. A.; Martínez, E.; Samitier, J. *Langmuir* **2007**, *23* (16), 8614−8618.

(27) Schlapak, R.; Danzberger, J.; Haselgrübler, T.; Hinterdorfer, P.; Schäffler, F.; Howorka, S. *Nano Lett.* **2012**, *12* (4), 1983−1989.

(28) Reynolds, N. P.; Tucker, J. D.; Davison, P. A.; Timney, J. A.; Hunter, C. N.; Leggett, G. J. *J. Am. Chem. Soc.* **2009**, *131* (3), 896−897.

DOI: 10.1021/acs.analchem.8b02588
Anal. Chem. 2018, 90, 12372−12376

(29) Wiesbauer, M.; Wollhofen, R.; Vasic, B.; Schilcher, K.; Jacak, J.; Klar, T. A. *Nano Lett.* **2013**, *13* (11), 5672−5678.
(30) Wolfesberger, C.; Wollhofen, R.; Buchegger, B.; Jacak, J.; Klar, T. A. *J. Nanobiotechnol.* **2015**, *13* (1), 27.
(31) Arnold, M.; Schwieder, M.; Blümmel, J.; Cavalcanti-Adam, E. A.; López-Garcia, M.; Kessler, H.; Geiger, B.; Spatz, J. P. *Soft Matter* **2009**, *5* (1), 72−77.
(32) Pi, F.; Dillard, P.; Alameddine, R.; Benard, E.; Wahl, A.; Ozerov, I.; Charrier, A.; Limozin, L.; Sengupta, K. *Nano Lett.* **2015**, *15* (8), 5178−5184.
(33) Schwarzenbacher, M.; Kaltenbrunner, M.; Brameshuber, M.; Hesch, C.; Paster, W.; Weghuber, J.; Heise, B.; Sonnleitner, A.; Stockinger, H.; Schütz, G. J. *Nat. Methods* **2008**, *5* (12), 1053−1060.
(34) Sevcsik, E.; Brameshuber, M.; Fölser, M.; Weghuber, J.; Honigmann, A.; Schütz, G. J. *Nat. Commun.* **2015**, *6*, 6969.
(35) Lohmüller, T.; Triffo, S.; O'Donoghue, G. P.; Xu, Q.; Coyle, M. P.; Groves, J. T. *Nano Lett.* **2011**, *11* (11), 4912−4918.
(36) Lohmüller, T.; Xu, Q.; Groves, J. T. *Nano Lett.* **2013**, *13* (7), 3059−3064.
(37) Narui, Y.; Salaita, K. S. *Chem. Sci.* **2012**, *3* (3), 794−799.
(38) Cai, H.; Muller, J.; Depoil, D.; Mayya, V.; Sheetz, M. P.; Dustin, M. L.; Wind, S. J. *Nat. Nanotechnol.* **2018**, *13*, 610.
(39) Dulkeith, E.; Morteani, A. C.; Niedereichholz, T.; Klar, T. A.; Feldmann, J.; Levi, S. A.; van Veggel, F. C. J. M.; Reinhoudt, D. N.; Möller, M.; Gittins, D. I. *Phys. Rev. Lett.* **2002**, *89* (20), 203002.
(40) Deeg, J.; Axmann, M.; Matic, J.; Liapis, A.; Depoil, D.; Afrose, J.; Curado, S.; Dustin, M. L.; Spatz, J. P. *Nano Lett.* **2013**, *13* (11), 5619−5626.
(41) Maruo, S.; Nakamura, O.; Kawata, S. *Opt. Lett.* **1997**, *22* (2), 132−134.
(42) Kawata, S.; Sun, H. B.; Tanaka, T.; Takada, K. *Nature* **2001**, *412* (6848), 697−698.
(43) Wollhofen, R.; Axmann, M.; Freudenthaler, P.; Gabriel, C.; Röhrl, C.; Stangl, H.; Klar, T. A.; Jacak, J. *ACS Appl. Mater. Interfaces* **2018**, *10* (2), 1474−1479.
(44) Li, L.; Fourkas, J. T. *Mater. Today* **2007**, *10* (6), 30−37.
(45) Farsari, M.; Vamvakaki, M.; Chichkov, B. N. *J. Opt.* **2010**, *12* (12), 124001.
(46) Cicha, K.; Li, Z.; Stadlmann, K.; Ovsianikov, A.; Markut-Kohl, R.; Liska, R.; Stampfl, J. *J. Appl. Phys.* **2011**, *110* (6), 064911.
(47) Fischer, J.; Wegener, M. *Opt. Mater. Express* **2011**, *1* (4), 614−624.
(48) Wollhofen, R.; Buchegger, B.; Eder, C.; Jacak, J.; Kreutzer, J.; Klar, T. A. *Opt. Mater. Express* **2017**, *7* (7), 2538−2559.
(49) Huppa, J. B.; Axmann, M.; Mörtelmaier, M. A.; Lillemeier, B. F.; Newell, E. W.; Brameshuber, M.; Klein, L. O.; Schütz, G. J.; Davis, M. M. *Nature* **2010**, *463* (7283), 963−967.
(50) Buchegger, B.; Kreutzer, J.; Plochberger, B.; Wollhofen, R.; Sivun, D.; Jacak, J.; Schütz, G. J.; Schubert, U.; Klar, T. A. *ACS Nano* **2016**, *10* (2), 1954−1959.
(51) Plochberger, B.; Stockner, T.; Chiantia, S.; Brameshuber, M.; Weghuber, J.; Hermetter, A.; Schwille, P.; Schütz, G. J. *Langmuir* **2010**, *26* (22), 17322−17329.
(52) Haensch, C.; Hoeppener, S.; Schubert, U. S. *Chem. Soc. Rev.* **2010**, *39* (6), 2323−2334.
(53) Mostegel, F. H.; Ducker, R. E.; Rieger, P. H.; El Zubir, O.; Xia, S.; Radl, S. V.; Edler, M.; Cartron, M. L.; Hunter, C. N.; Leggett, G. J.; Griesser, T. *J. Mater. Chem. B* **2015**, *3* (21), 4431−4438.
(54) Chilkoti, A.; Stayton, P. S. *J. Am. Chem. Soc.* **1995**, *117* (43), 10622−10628.
(55) Bayer, E. A.; Ben-Hur, H.; Wilchek, M. *Anal. Biochem.* **1986**, *154* (1), 367−370.
(56) Wollhofen, R.; Katzmann, J.; Hrelescu, C.; Jacak, J.; Klar, T. A. *Opt. Express* **2013**, *21* (9), 10831−10840.

DOI: 10.1021/acs.analchem.8b02588
Anal. Chem. 2018, 90, 12372−12376